Pascal Richet (Ed.),
Encyclopedia of Glass Science, Technology, History, and Culture, Volume 1, Wiley 2021,
Chapter 5.4, p. 559-568.

5.4
Nucleation, Growth, and Crystallization in Inorganic Glasses

Edgar D. Zanotto[1], Jürn W. P. Schmelzer[2], and Vladimir M. Fokin[3]

[1] Center for Research, Technology, and Education in Vitreous Materials (CeRTEV), Department of Materials Engineering, Federal University of São Carlos, São Carlos, SP, Brazil

[2] Institut für Physik, Universität Rostock, Rostock, Germany

[3] Vavilov State Optical Institute, Saint Petersburg, Russia

1 Introduction

When any liquid is cooled below its equilibrium melting or *liquidus* temperature, one or several crystalline phases may form. This process takes place in two steps: the formation of clusters and their subsequent evolution to macroscopic crystals. The first step is denoted *nucleation*, and the second is *crystal growth*. The effect of simultaneous crystal nucleation and growth is denominated *crystallization*. Crystallization counteracts vitrification, the freezing of a melt into a glass. Upon heating, the same phenomenon results in glass devitrification.

Eight decades ago, G.W. Morey [1] stated that "Devitrification is the chief factor which limits the composition range of practical glasses, it is an ever-present danger in all glass manufacture and working, and takes place promptly with any error in composition or technique." The prevention of crystal nucleation and growth upon cooling of any liquid – or upon heating of gels – gives rise to a glass. On the other hand, the global acceleration of technological breakthroughs, marked by high-tech industrial processes and devices, requires materials with unusual microstructures and enhanced or novel properties, such as transparency, bioactivity, ionic conductivity, or machinability, sometimes combined with excellent dielectric, magnetic, chemical, mechanical, or thermal shock resistance.

To meet this demand, significant efforts have focused on the synthesis of new glasses and glass ceramics. In both cases, crystallization control plays such a decisive role that reliable models of crystallization processes are needed. Hence, knowledge about the possible pathways of crystallization allows one to formulate kinetic criteria to answer the questions: "Under what conditions can a liquid supercool and transform into a glass, and under what conditions is substantial crystallization expected to occur on the cooling path?" In attempts to produce new glasses, crystal nucleation and growth must be avoided. Conversely, controlled crystallization can be used to synthesize fully crystallized materials or semicrystalline glass ceramics (Chapter 7.11). Several monographs provide detailed information on these materials (e.g. [2, 3]).

However, these technological aspects represent only one side of the widespread scientific interest in the kinetics of nucleation and crystallization in glasses. In addition to their practical relevance, glass-forming liquids serve as remarkable experimental models of metastable, highly viscous systems, in which crystallization and liquid–liquid phase separation processes can be quickly initiated, accelerated, or delayed. These processes can thus be studied conveniently under very different conditions on a laboratory timescale. Such analyses may even include the dependence of the kinetics of phase formation on the thermal history of the sample. For this reason, glass-forming liquids have served as *guinea pigs* for testing crystal nucleation and growth theories, providing a deeper insight into different phase formation processes. And lastly, crystallization produces impressive, uniquely beautiful (and frequently hidden) nano- and microstructures, as demonstrated by E.D. Zanotto [4], which serves as an additional motivation to join and pursue research in this endless, albeit highly gratifying quest to unveil the deeply hidden intricacies of glass crystallization and the resulting properties of glass ceramics.

To prevent or induce controlled crystal nucleation and growth in a glass requires some theoretical understanding of these complex phenomena. This chapter, therefore, outlines the basic fundamental aspects of the theory of crystallization of supercooled inorganic glass-forming liquids. Section 2 begins with a description of crystal nucleation kinetics, followed in Section 3 by an overview of some basic modes of crystal growth. Section 4 describes overall crystallization kinetics, i.e. the evolution of the volume fraction of crystalline phases as a function of time by nucleation and growth. In addition to some well-established results, we also briefly discuss some open problems and possible approaches to their resolution. A summary of relevant results and perspectives for future developments (Section 5) completes this chapter.

Pascal Richet (Ed.),
Encyclopedia of Glass Science, Technology, History, and Culture, Volume 1, Wiley 2021,
Chapter 5.4, p. 559-568.

2 Crystal Nucleation and Classical Nucleation Theory

The physical nature of nucleation phenomena in general and crystal nucleation in supercooled liquids in particular was first established and described by J.W. Gibbs [5]. His basic idea can be illustrated by the following approximation for the change of Gibbs free energy, ΔG, during crystal cluster formation:

$$\Delta G = -n\,\Delta\mu + \sigma A, \Delta\mu = \mu_l - \mu_{cr}, A = 4\pi R^2, n = \frac{4\pi}{3} c_\alpha R^3. \quad (1)$$

In formulating Eq. (1), it is assumed that spherical crystalline nuclei form in an initially homogeneous liquid. These nuclei are described by their radius, R; surface area, A; and the number, n, of particles (atoms, molecules, or more generally the basic structural units of the crystalline phase) they contain. In Eq. (1), $\Delta\mu$ is the difference of the chemical potentials per particle in the liquid (μ_l) and the crystal (μ_{cr}), σ is the specific interfacial energy, and c_α is the particle number density in the crystal cluster. From the specification of the parameters, it is evident that Eq. (1) is valid only for the simplest case of crystallization when liquid and crystal consist of the same structural units. This kind of crystallization is denoted as *congruent*. Also, it is assumed here that the state of the crystal clusters is independent of their sizes. Qualitatively, the situation does not change in general cases of *incongruent* crystallization, when the crystal and liquid phases have different compositions.

According to thermodynamic evolution criteria, at constant pressure, P, and temperature, T, spontaneous macroscopic processes are tied to a decrease in the Gibbs free energy, G, of the system. For this reason, if $\mu_l < \mu_{cr}$ and $\Delta\mu = (\mu_l - \mu_{cr}) < 0$, ΔG in Eq. (1) is a monotonically increasing function of cluster size for any possible values of R, so that crystal clusters of any size will disappear over time. The function $\Delta G = \Delta G(R)$ takes on the shape shown in Figure 1a only if the thermodynamic driving force for crystallization, $\Delta\mu$, is positive ($\mu_{cr} < \mu_l$). In this case, cluster formation and growth are accompanied by a decrease in the Gibbs free energy if the surface term in the expression for ΔG is neglected. However, this tendency for decreasing Gibbs free energy is counteracted by the surface term, i.e. the surface contribution to Gibbs free energy initially leads to an increase in ΔG with increasing crystal size. Small crystal clusters formed in the system disappear, and only clusters larger than a critical size, R_c, can grow to macroscopic dimensions. As demonstrated in Figure 1a, the critical cluster size is defined by the maximum of $\Delta G(R)$. Systems showing such behavior are denoted as metastable. Metastable states are stable with respect to small fluctuations (generating clusters with sizes $R < R_c$) but unstable with respect to larger fluctuations (leading to clusters with sizes $R > R_c$). Thus, viable (supercritical) crystal clusters capable of deterministic growth must exceed a critical size. It is this criticality that determines the crucial impact of these embryos of the newly evolving phase on the nucleation processes.

Taking the chemical potential difference and the specific interfacial energy as constants (i.e. employing the so-called "capillarity" approximation), one can derive the critical cluster size and the value of ΔG_c at the critical size from the extremum condition $d(\Delta G)/dT = 0$. These parameters are given by

$$R_c = \frac{2\sigma}{c_\alpha \Delta\mu}, \Delta G_c = \frac{1}{3}\sigma A_c = \frac{16\pi}{3}\frac{\sigma^3}{(c_\alpha \Delta\mu)^2}, A_c = 4\pi R_c^2. \quad (2)$$

These relations remain valid if more accurate expressions for $\Delta\mu$ are employed and the curvature dependence of the interfacial energy is accounted for. The concepts discussed above are illustrated in Figure 1a within the framework of the classical model of nucleation, whereby the change in the Gibbs free energy of cluster formation reaches a maximum $\Delta G = \Delta G_c$ for the critical cluster size, $R = R_c$. In this model, the clusters grow or decay while preserving their properties, so size is the only parameter specifying the state of the cluster.

A more realistic picture of cluster formation is presented in Figure 1b, where not only the size but also the composition (described by the number of particles, n_i, of two components) of the cluster may change. In this case, the critical cluster corresponds to a saddle point of the Gibbs free energy surface. The evolution to the new phase via the saddle is shown by the dark (red in the colored version) curve. In Figure 1c, we show an alternative to the classical picture of phase evolution, which is similar to spinodal decomposition (cf. [3]). In this case, the composition of the critical crystal cluster changes retaining a nearly constant size and only after completion of this process the kinetics are governed by the growth of clusters with a roughly constant composition. In a variety of cases in multicomponent systems [3], the latter path of evolution (Figure 1c) – and not the classical picture (Figure 1a) – dominates phase formation.

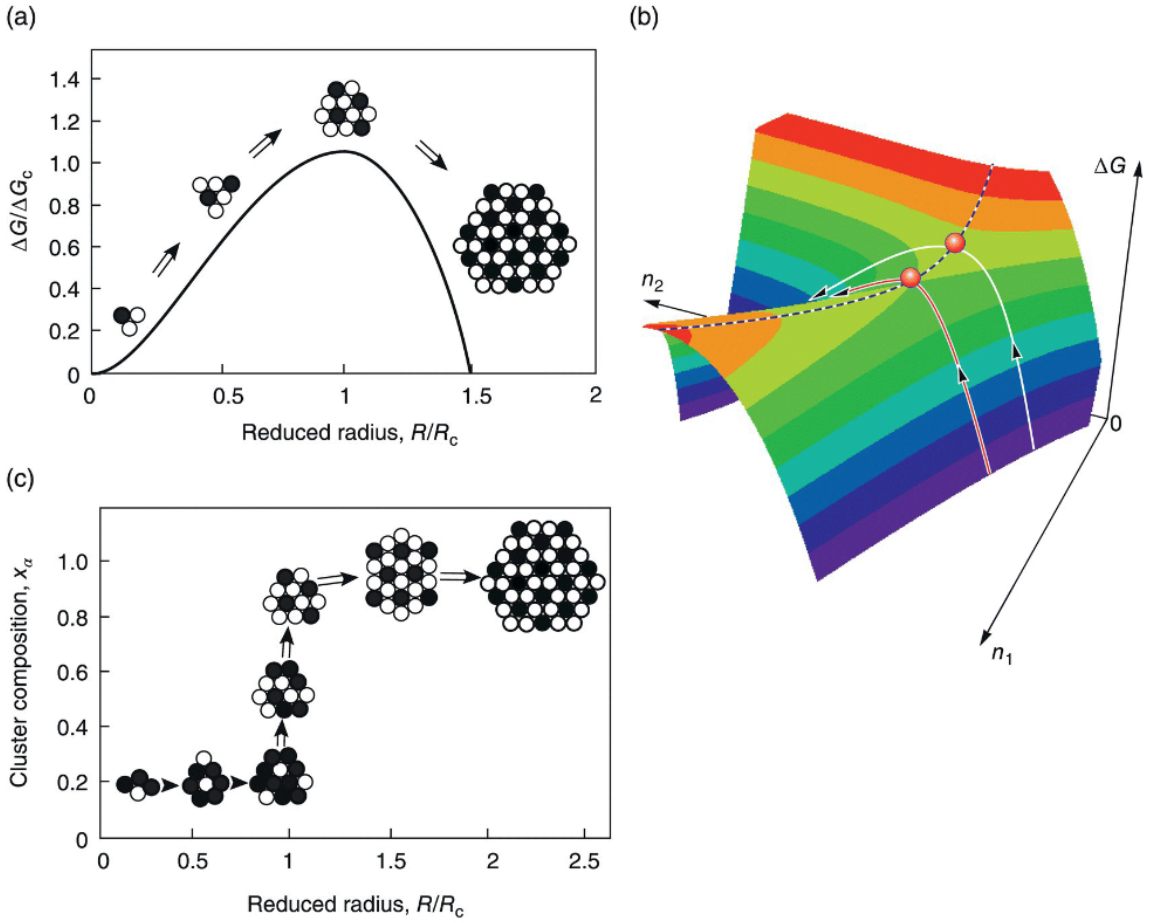

Figure 1 The classical model of nucleation and possible generalizations. (a) With only one parameter employed to describe the state of the cluster. (b) Change of Gibbs free energy in cluster formation when more than one parameter is used. (c) Alternative to the classical scenario of crystallization in multicomponent liquids .

Critical clusters do not form according to the predictions (the evolution criteria) of macroscopic thermodynamics, but instead by stochastic thermal fluctuations. According to underlying assumptions of statistical physics, the probability of such fluctuations can be expressed as a function of the minimum work for a reversible thermodynamic process. The minimum work to form a critical cluster is $W_c = \Delta G_c$, where ΔG_c is given by Eq. (2). This quantity, W_c, the work of critical cluster formation, plays a decisive role in nucleation theory. Initially, the nucleation rate is small. Then, after a certain time interval, τ, the so-called time lag for nucleation, the rate of nucleation, J (i.e. the number of supercritical clusters formed per unit time in a unit volume of the liquid), approaches a constant value, the steady-state nucleation rate, J_s. In an early description of this initial period of nucleation by Zeldovich (cf. [3]), the nucleation rate as a function of time, t, was expressed by the relation

$$J(t) = J_s \exp\left(-\frac{\tau}{t}\right). \tag{3}$$

The initial stage of nucleation observed in experiments is often described by the Collins–Kashchiev relation (cf. [3]):

$$N(t) = J_s\tau\left[\frac{t}{\tau} - \frac{\pi^2}{6} - 2\sum_{m=1}^{\infty}\frac{(-1)^m}{m^2}\exp\left(-m^2\frac{t}{\tau}\right)\right]. \tag{4}$$

This mathematical equation gives a relation for the number, $N(t)$, of supercritical crystallites as a function on time, t. For longer times than some induction time ($t \gg t_{ind}$), Eq. (4) can be approximated by

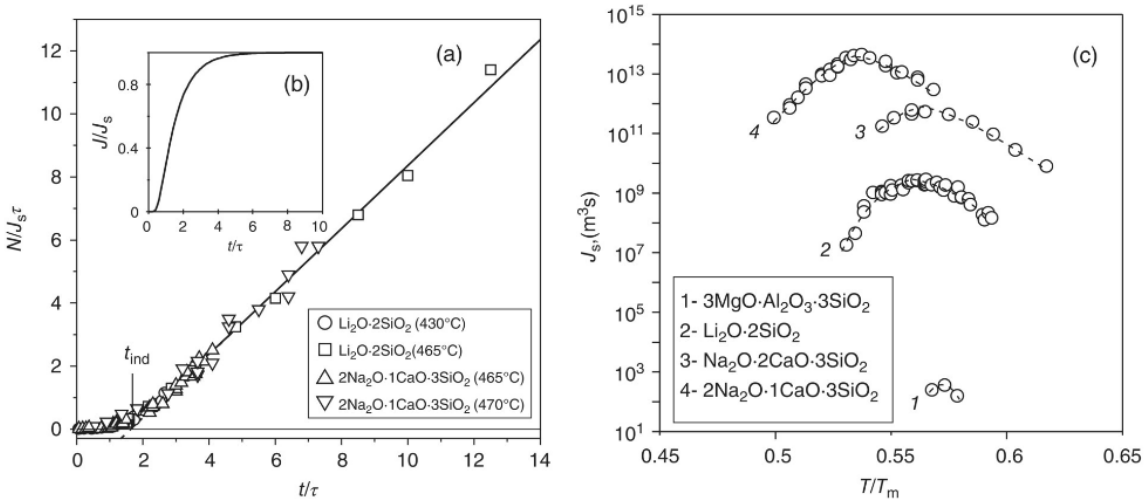

Figure 2 Experimental nucleation rate data for several silicate glasses. (a) Reduced crystal number density, $(N(t)/J_s\,\tau)$, versus reduced nucleation time, (t/τ). The solid line is the master curve calculated from Eq. (4). (b) Reduced nucleation rate versus reduced nucleation time calculated from Eq. (4). (c) Experimental steady-state nucleation rate, J_s, versus reduced temperature, T/T_m, for four stoichiometric glasses. T_m is the melting temperature (see [6] for details).

$$N(t) \cong J_s(t - t_{ind}), \quad t_{ind} = \frac{\pi^2}{6}\tau. \tag{5}$$

where τ is the nucleation time lag. Over a sufficiently large timescale, Eqs. approach steady-state nucleation conditions, i.e. $(dN/dt) = J_s$ = constant. With $W_c = \Delta G_c$, the steady-state nucleation rate, J_s, can be written as [3]

$$J_s = J_0 \exp\left(-\frac{\Delta G_c}{k_B T}\right) = J_0 \exp\left(-\frac{W_c}{k_B T}\right), J_0 = \sqrt{\frac{\sigma}{k_B T}}\left(\frac{D}{d_0^4}\right), \tag{6}$$

where D is an appropriately chosen diffusion coefficient and d_0 is a size parameter explained in greater detail below. Experimental results that illustrate the establishment of a steady-state nucleation rate and its dependence on temperature are shown in Figure 2.

For the case shown in Figure 1a (congruent crystallization, assuming that the state of the cluster does not change with size and is the same as that of the newly evolving macroscopic phase), D in Eq. (6) is the diffusion coefficient of the structural building units in the liquid, and d_0 is their diameter. If several components of the liquid diffuse independently, D must be replaced by an effective diffusion coefficient, which is a combination of the partial diffusion coefficients and the concentrations of the different components in the liquid, and d_0 must be replaced by the average size of these independently moving species [3].

In the application of the theory, it is also often assumed that the effective diffusion coefficient can be replaced by the Newtonian shear viscosity, η, via the Stokes–Einstein–Eyring (SEE) equation [3]:

$$D \cong \frac{k_B T}{d_0 \eta}. \tag{7}$$

However, its applicability to states near and below the glass transition temperature (where homogeneous crystal nucleation is commonly observable) has been questioned even for "one-component" congruent systems, where decoupling of relaxation (expressed by viscosity) and atomic transport (represented by the diffusion coefficient) is frequently reported (e.g. [7]). Application of this expression is even more questionable for multicomponent systems. Another issue is related to the case of highly viscous glass-forming melts, for which a non-Newtonian viscosity should be employed to describe viscous flow [3]. Leaving aside the reservations above, by applying the SEE relationship, one arrives at the following expression for the steady-state nucleation rate:

$$J_s = \frac{\sqrt{\sigma k_B T}}{d_0^5 \eta} \exp\left(-\frac{\Delta G_c}{k_B T}\right). \quad (8)$$

To apply Eq. (8) to the interpretation of experimental data, one has to determine the work of critical cluster formation, $W_c = \Delta G_c$, i.e. to specify the thermodynamic driving force of phase formation, $\Delta\mu$, and the specific interfacial energy, σ in Eq. (2). Assuming that the bulk properties of the crystal clusters are the same as those of the macroscopic crystals, one arrives at the simplest approximation by a Taylor expansion of $\Delta\mu(T)$ in the vicinity of the melting temperature:

$$\Delta\mu(T) = \Delta h_m \left(1 - \frac{T}{T_m}\right), \quad (9)$$

where Δh_m is the enthalpy of melting per structural unit of the crystal and T_m is the melting temperature (generalizations of this relation can be found in [3]).

Since the interfacial energy of the critical nucleus is not directly measurable, it is normally evaluated using the Stefan–Skapski–Turnbull rule [3]:

$$\sigma = \varsigma \frac{q_m}{N_A^{1/3} v_m^{2/3}}, \quad q_m = N_A \Delta h_m, \quad (10)$$

via the molar enthalpy of melting, q_m. In Eq. (10), N_A is Avogadro's number, ς is a factor varying from 0.4 to 0.6, and v_m is the molar volume. This relation has been widely employed (see [3] and Baidakov et al. [8]). By substituting these relations into the expression for the steady-state nucleation rate, its temperature dependence can be interpreted straightforwardly. The steady-state nucleation rate J_s is equal to zero at $T = T_m$, where $\Delta\mu = 0$, cf. Eq. (9). This rate increases with decreasing temperature because of the decrease in the work of critical cluster formation borne out by Eq. (2), until this trend is overcompensated by the exponential increase in viscosity with decreasing temperature.

When these classical concepts are employed to interpret experimental data, a qualitative and partly quantitative agreement is sometimes found (cf. Figure 2). In most cases, however, the classical approach underestimates the steady-state nucleation rates by 20–55 orders of magnitude, e.g. [6]. In the classical approach, the deviations between experiment and theory can be (artificially) resolved by the introduction of a size dependence of the specific interfacial energy, as discussed by Gibbs [5] and later by others, particularly by Tolman (cf. [3]). But this type of solution gives rise to other problems [6]. Another possible solution, in agreement with results of computer simulations and density functional computations, consists in accounting for the size dependence not only of the surface but also of the bulk properties of the clusters of the newly evolving phases. The bulk properties of the clusters generally depend on their sizes. Hence, the surface properties, including the surface tension, must also be size dependent. Thus, this approach also leads to a size dependence of the surface energy, but the primary variation of the properties of the clusters lies in the size dependence of their bulk properties.

Thermodynamically, one can treat these problems by generalizing the classical Gibbs approach (cf. [3]), which allows for a description of the cluster properties as a function of size and degree of supercooling. With this new thermodynamic (generalized Gibbs) approach, one concludes that the classical theory – assuming macroscopic bulk properties of the clusters and employing the capillarity approximation for the specific interfacial energy – overestimates the work of critical cluster formation, and hence, underestimates the values of steady-state nucleation rates [3]. Therefore, the classical theory with the “capillarity” approximation may serve as a tool for roughly estimating the nucleation rate curve (i.e. its dependence on temperature and/or pressure), but it must be improved to account for the above-specified effects for a detailed and quantitatively accurate description of the phenomenon.

So far, we have considered the case of crystal nuclei that form evenly within a pure liquid. This mechanism is known as *homogeneous* nucleation. However, nucleation can be readily catalyzed by impurities, such as solid particles embedded in the volume or present on the external surface of glasses. Nucleation originating at such preferential sites is denoted as *heterogeneous* (e.g. [3, 9]) and can be described by the theoretical concepts outlined above if the work of critical cluster formation for homogeneous nucleation, W_c, is replaced by $W_c\Phi$. Here, $\Phi \leq 1$ is the nucleating activity of the heterogeneous nucleation core, and its value depends on the mechanism of nucleation catalysis. As a rule, heterogeneous nucleation dominates at small supercooling because of the lower work of critical cluster formation than that of homogeneous nucleation. At high supercooling, homogeneous nucleation dominates due to the much larger number of sites (all “molecules” of the system) where homogeneous nucleation may proceed.

The reader should note that, in certain cases, the evolution of the new phase may not proceed via the saddle shown as a dark curve in Figure 1b (in red in the colored version) but via a ridge trajectory indicated by a light curve in Figure 1b (in yellow in the colored version), if such a trajectory is kinetically favored. This type of behavior may be expected to occur in crystallization occurring at large degrees of supercooling because of the disordered and nonstoichiometric nature of the crystals that precipitate in the early stages.

Frequently, several different stable or metastable phases may be formed at some given initial state of the supercooled liquid. As Ostwald suggested (cf. [3]), in such cases the most favorable stable phase is not formed immediately. Instead, the final stable phase is reached via several stages in which different metastable phases are formed until the most stable phase is developed: this is the so-called Ostwald's rule of stages or Ostwald's step rule. As first proposed by Stranski and Totomanov (cf. [3]), this evolution path can also be explained by kinetic considerations.

3 Basic Models of Crystal Growth in Supercooled Liquids

It is now generally accepted that the properties of the crystal–liquid interface have a decisive influence on the kinetics of crystallization. Theoretical treatments of crystal growth have therefore focused closely on the interfacial structure and its effect on crystallization. With the assumption of congruent crystallization, three standard models have been developed for treating crystal growth theoretically (e.g. [10, 11]). These models are described briefly below:

i. *Normal growth:* The interface is pictured as rough at an atomic scale. Growth takes place at step sites, which represent a sizable fraction (0.5–1.0) of the interface. Assuming that this fraction does not change appreciably with temperature, the growth rate, $u(T)$, can be expressed as

$$u = f\frac{D}{4d_0}\left[1 - \exp\left(-\frac{\Delta\mu}{k_B T}\right)\right], \tag{11}$$

where f is close to unity and $\Delta\mu$ is treated as a positive quantity.

ii. *Screw dislocation growth:* This model assumes the interface is smooth but imperfect at an atomic scale. Growth takes place at a few step sites provided by screw dislocations that intersect the interface. The growth rate is still given by Eq. (11), where f is now the fraction of preferred growth sites (on the dislocation ledges) at the interface. In this case, f is given approximately by $f \simeq (T_m - T)/(2\pi T_m)$ [7]. More generally, according to Jackson [10], $f = (\Delta s_m/k_B)\xi$ holds, where Δs_m is the entropy of fusion per particle and ξ is the number of nearest-neighbor sites in a layer parallel to the surface divided by the total number of nearest-neighbor sites. Factor ξ is the largest for the most closely packed planes of the crystal, for which it is approximately equal to 0.5.

For $f < 2$, the minimum free energy configuration corresponds to half the available sites being filled and represents an atomically rough surface. In contrast, for $f > 2$, the lowest free energy configuration corresponds to a surface where few sites are filled and a few units are missing from the completed layer, which represents an atomically smooth interface. Hence, for materials with $\Delta s_m < 2k_B$, the most closely packed interface planes should be rough. For materials with $\Delta s_m > 4k_B$, the most closely packed surfaces should be smooth, the less tightly packed surfaces rough, and the growth anisotropy rate large.

iii. *Surface nucleation or two-dimensional growth*: According to this model, the interface is smooth and perfect at an atomic scale and thus free of intersecting screw dislocations and growth sites. Growth then takes place by the formation and growth of new two-dimensional nuclei at the interface. In this case, the growth rate is expressed by

$$u = C_3\frac{D}{4d_0^2}\exp\left(-\frac{C_2}{T\Delta T}\right), \tag{12}$$

where C_2 and C_3 are parameters that determine the time required for the formation of the two-dimensional nucleus relative to that required for its propagation across the interface, respectively.

Possible growth modes are illustrated in Figure 3. Similarly to nucleation, the interplay between increasing driving force for crystallization, $\Delta\mu$, and decreasing diffusion coefficient (or increase in viscosity) with decreasing temperature results in a maximum of the crystal growth rates. This maximum is located at higher temperatures than that of the maximum of the steady-state nucleation rate shown in Figure 2c.

There are also other growth modes, which are rate limited not by processes at the liquid–crystal interface but by mass transport toward the interface. A specific example is a diffusion-limited segregation, which is of particular importance in multicomponent systems. Accounting for size effects on the growth kinetics, one can express the rate for such a growth mode as (e.g. [11, 12])

$$\frac{dR}{dt} = \frac{B}{R}\left(\frac{1}{R_c} - \frac{1}{R}\right), \tag{13}$$

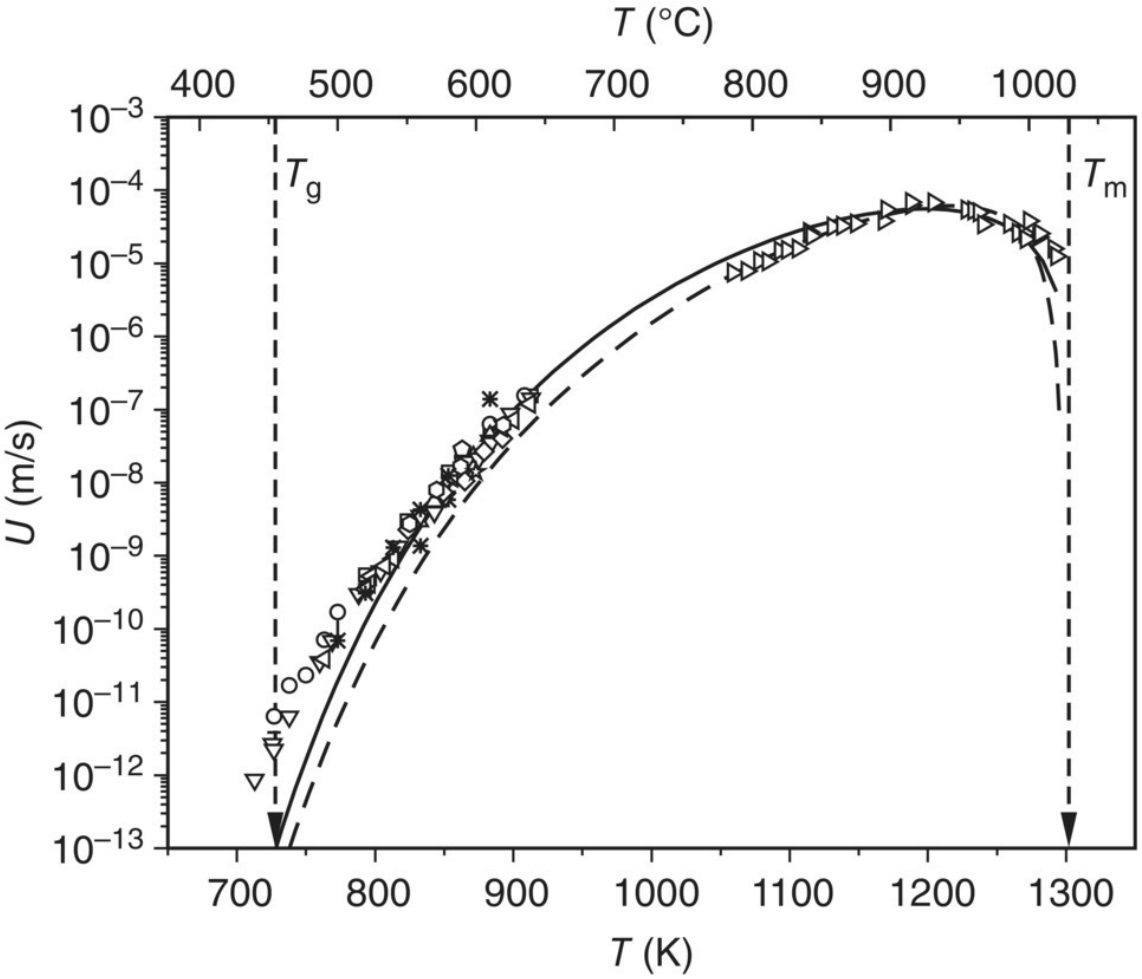

Figure 3 Crystal growth rates for $Li_2O{\cdot}2SiO_2$ glasses obtained by different authors. The lines correspond to the screw dislocation mechanism (full curve) and two-dimensional surface nucleated growth (dashed curve) [7].

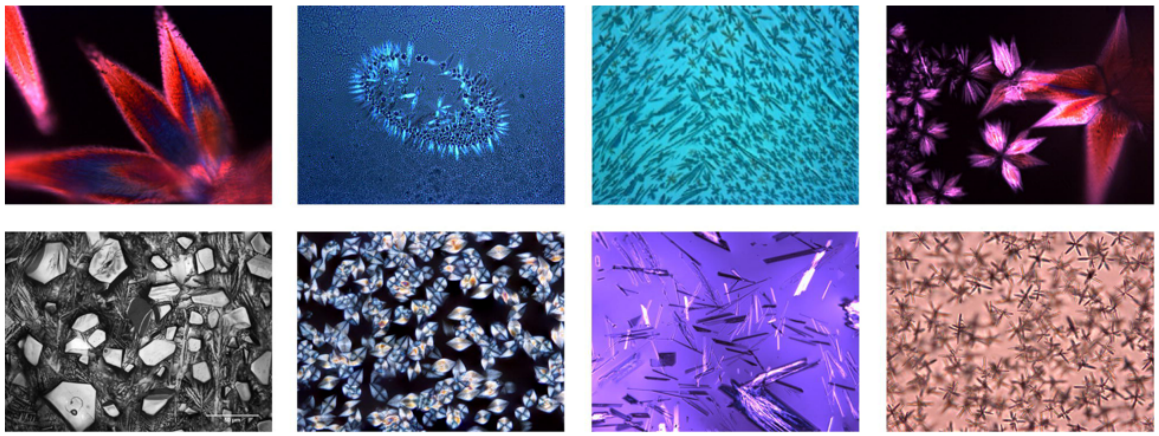

Figure 4 Crystal morphologies formed by nucleation and growth in glass-forming liquids as observed by optical microscopy (crystal sizes from 5 to 100 μm). From top left to bottom right: (i, ii, iv) LS crystals nucleated on defects of a $CaO{\cdot}Li_2O{\cdot}SiO_2$ glass surface during its preparation via melting–cooling. (iii) Crystallization propagating from the surface toward the center of a $CaO{\cdot}Li_2O{\cdot}SiO_2$ glass specimen; lithium metasilicate crystals nucleated on two perpendicular

surfaces and grew toward the sample center. (v) Surface of a $CaO{\cdot}Li_2O{\cdot}SiO_2$ glass sample after cooling a melt in a DSC furnace; the large-faceted and needle-like crystals are calcium and lithium metasilicates, respectively. (vi) Internal crystallization in a Ti-cordierite glass; pure stoichiometric cordierite ($2MgO{\cdot}2Al_2O{\cdot}5SiO_2$) glass underwent only surface nucleation, but the same glass doped with more than 6 mol % TiO_2 shows internal crystallization of μ-cordierite. (vii) Needle-like crystals in $CaO{\cdot}Li_2O{\cdot}SiO_2$ eutectic glass formed by internal crystallization in the temperature range between the *solidus* and the *liquidus;* these wollastonite crystals appear on the cooling path. (viii) Starlike NaF crystals inside a PTR glass (treatment at a high temperature near the solubility limit).

where B is a combination of parameters describing the liquid under consideration, being proportional to the effective diffusion coefficient governing the rate of supply of the different components to the growing or dissolving cluster.

Equation (13) and its modifications for other growth modes serve as a basis for the theoretical description of the competitive growth of clusters denoted as coarsening or Ostwald ripening. In these late stages of phase formation, larger clusters may grow further only when subcritical crystals are dissolved. The theoretical description of this process was first developed by Lifshitz and Slezov (cf. [11]). Today it is often referred to as the Lifshitz–Slezov–Wagner theory. This theory provides expressions for the average size, $\langle R\rangle$, and the number, N, of supercritical clusters in the system as a function of time. For diffusion-limited growth (Eq. (13)), one obtains

$$\langle R\rangle^3 \propto t, \quad N \propto \frac{1}{t}. \tag{14}$$

An account of the effect of elastic stresses on coarsening, which leads to qualitative modifications of the coarsening behavior, is reviewed in [3, 12].

The above relationships allow one to describe the growth of crystals with smooth planar or spherical interfaces advancing in the liquid. However, more complex growth patterns do exist, and more complex models of growth are required to properly take into account possible interfacial instabilities, surface roughening, or other growth modes such as diffusion-limited aggregation [11]. With such complex growth modes, a variety of intricate and beautiful crystal shapes may evolve, some of which are illustrated in Figure 4.

4 Overall Crystallization and Glass-forming Ability: The Johnson–Mehl–Avrami–Kolmogorov Approach

The overall crystallization of supercooled liquids occurs by a combination of crystal nucleation and growth. The kinetics of such processes is usually described by a theory independently derived between 1937 and 1941 by Johnson, Mehl, Avrami, and Kolmogorov [13–17] (JMAK theory). In this approach, the evolution of the total amount of crystalline phase is described as a function of time, accounting simultaneously for nucleation and growth. The basic equations of this approach can be developed as follows.

Let us assume that, in a time interval $dt'(t', t' + dt')$, a number $dN(t') = J(t')[V - V_n(t')]$ of clusters of critical size is formed in the volume $[V - V_n(t')]$. Here, V is the initial volume of the glass-forming melt and $V_n(t')$ the volume already crystallized at time t'. These clusters grow and, at time t, occupy a volume

$$dV_n(t,t') = \omega_n J(t')(V - V_n(t'))dt'\left(\int_{t'}^{t} u(t'')dt''\right)^n, \tag{15}$$

where ω_n is a shape factor and the integral term describes the growth of the $dN(t')$ clusters formed at t' until time t, i.e. in the time interval $(t–t')$, the exponent n is the number of independent spatial directions of growth. Introducing the ratio, $\alpha_n(t) = (V_n(t)/V)$, between the current volume of the crystalline phase versus the initial volume of the glass-forming melt, one has

$$d\alpha_n(t,t') = \omega_n J(t')(1 - \alpha_n(t'))dt'\left(\int_{t'}^{t} u(t'')dt''\right)^n. \tag{16}$$

Integration, i.e. taking the sum over all the time intervals dt' in the range of $(0, t)$, yields

$$\alpha_n(t) = 1 - \exp\left(\omega_n \int_0^t J(t')\mathrm{d}t' \left(\int_{t'}^t u(t'')\mathrm{d}t''\right)^n\right). \quad (17)$$

Provided the nucleation and growth rates are both constant, one reaches as a special case

$$\alpha_n(t) = 1 - \exp\left(-\frac{\omega_n}{(n+1)} J u^n t^{(n+1)}\right). \quad (18)$$

Conversely, if a number N_0 of supercritical clusters is formed immediately at time $t = 0$, growing in n independent spatial directions, one arrives instead at

$$\alpha_n(t) = 1 - \exp\left(-gN_0 u^n t^n\right). \quad (19)$$

The analysis of the time dependence of the $\alpha_n(t)$-curves thus leads one to the specification of nucleation and growth kinetics.

The JMAK theory has been employed in numerous studies to analyze experimental data and determine the degree of crystallinity as a function of time in both isothermal and non-isothermal heat treatments of glass systems. Emphasis has usually been given to the determination of the so-called Avrami coefficient $m = n + 1$ obtained from the slopes of experimental $\ln[\ln(1 - \alpha)^{-1}]$ versus $\ln(t)$ plots. An overview of various nucleation and growth mechanisms and the resulting values of the Avrami coefficient are given in [3]. However, there is some uncertainty in such analyses, because different combinations of nucleation and growth laws may lead to the same Avrami coefficient. For this reason, a separate investigation of the growth kinetics may be required to reach definite conclusions [14].

It is important to underline that the JMAK theory, as given by Eqs. (18) and (19), does not apply to non-isothermal processes. These two equations are derived from the assumption of constant nucleation and growth rates, which are not achieved in non-isothermal processes. Therefore, in non-isothermal cases, the general relationships, Eqs. (16) and (17), must be employed to describe overall crystallization. This requires taking into consideration not only thermal nucleation (formation of supercritical clusters due to thermal fluctuations at given values of critical cluster size and thermodynamic barrier) but also athermal nucleation (i.e. the change in the number of supercritical clusters due to the variation of the critical cluster size resulting from the change in temperature).

Such considerations must also be taken into account when the JMAK formalism is employed to determine whether a liquid will transform into a glass upon cooling or whether it will crystallize. Following Uhlmann (cf. [10]), one can consider a supercooled frozen in liquid as a glass if, after vitrification, the volume fraction of the crystal phase does not exceed a certain value of, say, 10^{-6} (the detection limit by microscopy). Using appropriate expressions for nucleation and growth rates, one can then compute (through Eq. (18) for isothermal conditions) the time required to reach the volume fractions thus defined. In this way, one arrives at the so-called *T*(ime)*T*(emperature)*T*(ransformation) curves (*TTT* curves) exemplified in Figure 5 (cf. also [18] and figure 10.8 in [3]). These curves give some insight into the characteristic timescales required to prevent measurable crystallization effects. One should keep in mind, however, that these curves overestimate the critical cooling rates for glass formation by about one order of magnitude because, as mentioned earlier, crystallization upon cooling proceeds under non-isothermal conditions.

Using experimental nucleation and growth rate data, Rodrigues and Zanotto [19] calculated *TTT* curves for different isothermal and non-isothermal crystallization situations. They also accounted for the breakdown of the SEE equation at a temperature T_b (somewhat higher than T_g) where the effective diffusion coefficient that controls crystal growth decouples from the value of diffusivity calculated by the SEE equation (Eq. (7)). In Figure 5 we show an example of such a curve for a stoichiometric $BaO{\cdot}2TiO_2{\cdot}2SiO_2$ glass, which undergoes copious internal homogenous crystal nucleation. The agreement with experimental data (which, in this case, were also obtained in isothermal conditions) is quite impressive, indicating that the JMAK equation is accurate if all the assumptions involved in its derivation are met.

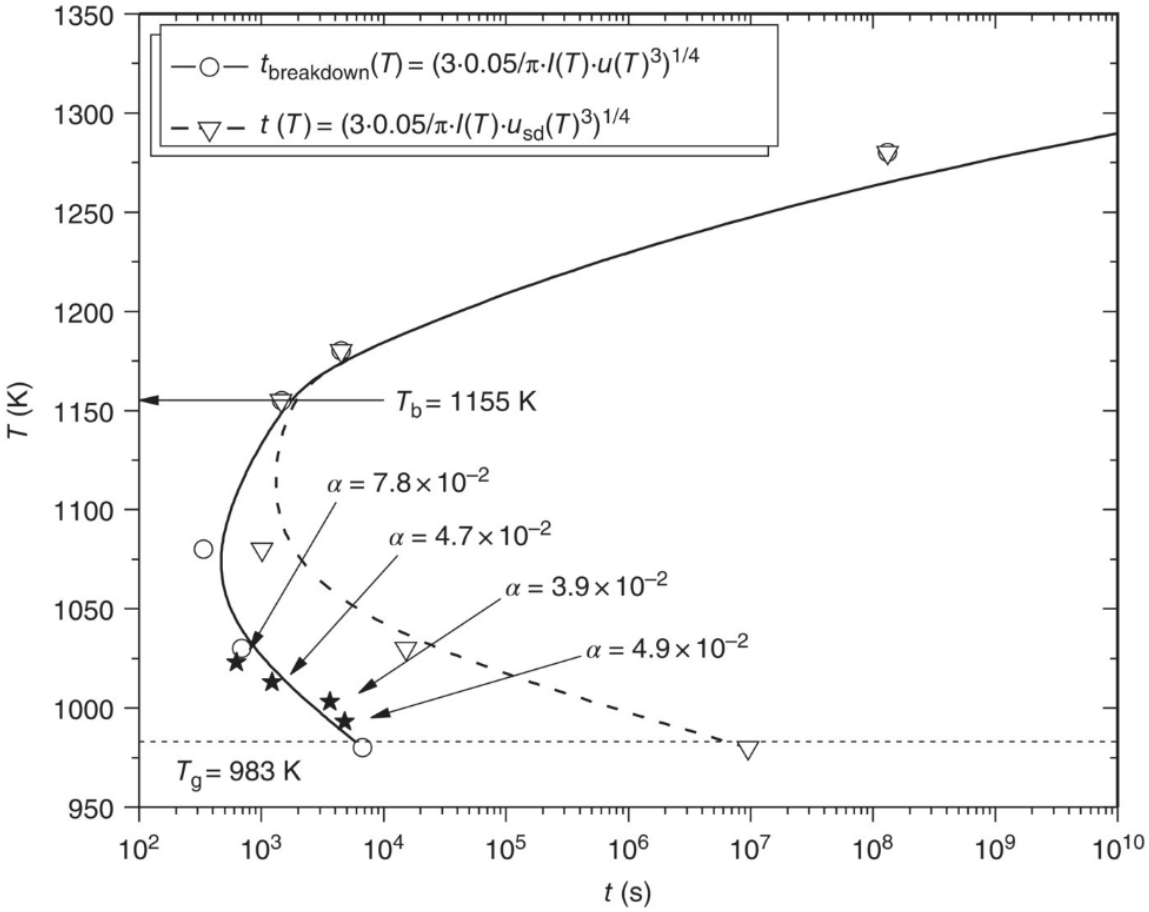

Figure 5 Simulated *TTT* curves for a $BaO{\cdot}2TiO_2{\cdot}2SiO_2$ glass with crystallized volume fraction α = 0.05 using, in one approach, the screw dislocation growth model both above and below T_b (t_{sd} – dashed line), and in the other the Arrhenius equation below T_b ($t_{breakdown}$ – solid line). Experimental data points (black stars) obtained at 993, 1003, 1013, and 1023 K [15].

5 Perspectives

Significant advances in the understanding and control of crystal nucleation and growth processes in glass-forming liquids have been achieved in the last five decades. It is now well-established that almost all materials can vitrify when subjected to sufficiently fast cooling from the liquid state. Thus, novel materials, such as metallic and chalcogenide glasses with unusual properties, have been obtained successfully by very fast quenching. Also, controlled, catalyzed internal crystallization of specific glasses has led to a variety of advanced glass ceramics that are now manufactured commercially. More profound insights into glass crystallization processes, such as precise predictions of nucleation and growth rates and critical cooling rates for glass formation, based solely on materials properties, will depend critically on new developments in nucleation and growth theories and computer simulations.

Despite the many advances achieved in understanding crystallization processes in glasses, some problems remain open. Among the most important, we remark the following: (i) specification of the bulk (structure, composition, density) and surface properties of the critical nuclei and sub- and supercritical crystals as a function of their sizes; (ii) description of the temperature dependence of the crystal nucleus–liquid interfacial energy and the degree of validity of the Stefan–Skapski–Turnbull equation; (iii) applicability of the SEE (viscosity) relationship in calculating the effective diffusion coefficients that control crystal nucleation and crystal growth; (vi) a clear understanding of the causes of the breakdown of the SEE equation reported for crystal growth somewhat above T_g; (v) unveiling the cause of the reported breakdown of the CNT in describing the temperature dependence of experimental nucleation rates below T_g; (vi) a deeper understanding of the relationship, if any, between the molecular structure of glass-forming melts and the nucleation and growth mechanisms [20]; (vii) the relation between the sizes of supercritical nuclei vis-à-vis the sizes of cooperatively rearranging regions (CRR) of the configurational entropy theory and the domains of heterogeneous dynamics (DHD) envisaged in the structure of viscous liquids [21]; and (viii) comparison of the estimated (by extrapolation) structural relaxation time and the

characteristic time for crystallization of glass-forming liquids at the (predicted) Kauzmann temperature, T_K [22, 23]. Such a comparison could resolve the paradox, following Kauzmann's suggestion of the possibility that the putative state of negative entropy may never be reached because crystallization would always intervene before structural relaxation. A detailed analysis of the Kauzmann paradox and his hypothesis about the existence of a kinetic spinodal has been performed recently [24]. In addition, the ratio of the mentioned times scales is of considerable importance concerning the problem whether some basic assumptions of CNT concerning the methods of determination of the thermodynamic driving force and the surface tension hold or not for crystallization under time-dependent temperature and/or pressure [25]. All these problems, in addition to several others not mentioned here, such as the development of novel glasses and glass ceramics, having exotic, unusual compositions and combination of properties, serve as great incitement for glass crystallization being a very active research topic!

Acknowledgments

The authors are indebted to their numerous co-workers and students for enjoyable and educative joint research in the past 40 years and to Profs. E. B. Ferreira and F. C. Serbena for their critical comments. Generous and continuous funding by the Brazilian agencies CAPES, CNPq, and São Paulo Research Foundation, FAPESP (CEPID grant # 13/07793-6), is much appreciated.

Table of Symbols

ΔG
: Gibbs free energy difference

R
: cluster radius

A
: nucleus surface area

N
: number density of supercritical crystallites

$\Delta\mu$
: chemical potential difference

μ_1
: the chemical potentials perparticle in the liquid

μ_{cr}
: the chemical potentials per particle in the crystal

σ
: surface free energy

c_α
: particle number density in the crystal cluster

P
: pressure

T
: temperature

G
: Gibbs free energy

R_c
: critical radius

ΔG_c
: change in the Gibbs free energy for a critical cluster

n_i
: number of particles of the different components in the cluster

W_c
: work of critical cluster formation

τ
: time-lag in nucleation

J
: rate of formation of supercritical clusters

J_s
steady-state nucleation rate

t
time

n_c
number of particles in a cluster of critical size

τ_R
Maxwellian relaxation time

η
Newtonian viscosity

t_{ind}
induction time

dN
change of number of clusters of critical size

dt
time interval

k_B
Boltzmann's constant

D
diffusion coefficient

d_o
diameter

T_m
melting temperature

Δh_m
heat of melting of one crystal phase particle

q_m
heat of melting

N_A
Avogadro's number

ς
correction factor

f
fraction of preferred growth sites

Δs_m
entropy of melting

C_2, C_3
parameters determining the time required for the formation of the two-dimensional nucleus and for its propagation across the interface, respectively.

B
combination of parameters proportional to the effective diffusion coefficient

$\langle R \rangle$
average size of the nuclei

dt'
time interval

V
volume

V_n
volume crystallized

ω_n
shape factor

$a_n(t) = (V_n(t)/V)$
time-dependent crystallized fraction

N_o
number of supercritical clusters

n
number of independent spatial directions

T_b
Stokes–Einstein breakdown temperature

T_g
glass transition temperature

T_K
Kauzmann temperature

Φ
catalytic activity factor of a heterogeneous nucleation core

References

1 Morey, G.W. (1938). *The Properties of Glass*, 1954. New York: Reinhold Publishers.

2 Höland, W. and Beall, G.H. (2013). *Glass-Ceramic Technology*, 2nd ed. Hoboken, NJ: Wiley.

3 Gutzow, I.S. and Schmelzer, J.W.P. (1995). *The Vitreous State: Thermodynamics, Structure, Rheology, and Crystallization*. Berlin: Springer; Heidelberg: Springer, 2nd enlarged ed., 2013.

4 Zanotto, E.D. (2013). *Crystals in Glass: A Hidden Beauty*. Hoboken, N.J: Wiley.

5 Gibbs, J.W. (1926). Collected works. In: *Thermodynamics*, vol. 1. New York: Longmans.

6 Fokin, V.M., Zanotto, E.D., Yuritsyn, N.S., and Schmelzer, J.W.P. (2006). Homogeneous crystal nucleation in silicate glasses: a 40 years perspective. *J. Non-Cryst. Solids* 352: 2681–2714.

7 Nascimento, M.L.F., Fokin, V.M., Zanotto, E.D., and Abyzov, A.S. (2011). Dynamic processes in a silicate liquid from above to below the glass transition. *J. Chem. Phys.* 135: 194703.

8 Baidakov, V.G., Protsenko, S.P., and Tipeev, A.O. (2013). Temperature dependence of the crystal-liquid interfacial free energy and the endpoint of the melting line. *J. Chem. Phys.* 139: 224703/1–224703/12.

9 Volmer, M. (1939). *Kinetik der Phasenbildung*. Th. Steinkopff: Dresden.

10 Uhlmann, D.R. (1982). Crystal growth in glass-forming liquids: a ten-year perspective. In: *Advances in Ceramics*, vol. 4 (eds. J.H. Simmons, D.R. Uhlmann and G.H. Beall), 80–124. Columbus: American Ceramic Society.

11 Jackson, K.A. (2004). *Kinetic Processes*. Weinheim: Wiley-VCH.

12 Slezov, V.V. (1999). *Kinetics of First-Order Phase Transitions*. Weinheim: Wiley-VCH.

13 Kolmogorov, A.N. (1937). On the statistical theory of crystallization of metals. *Izv. Akad. Nauk SSSR* 3: 355–359.

14 Johnson, W.A. and Mehl, R. (1939). Reaction kinetics in processes of nucleation and growth. *Trans. AIME* 135: 416–458.

15 Avrami, M. (1939). Kinetics of phase change. I. General theory. *J. Chem. Phys.* 7: 1103–1112.

16 Avrami, M. (1940). Kinetics of phase change. II. Transformation time relations for random distribution of nuclei. *J. Chem. Phys.* 8: 212–224.

17 Avrami, M. (1941). Kinetics of phase change. III. Granulation, phase change, and microstructure kinetics of phase change. *J. Chem. Phys.* 9: 177–184.

18 Kelton, K.F. and Greer, A.L. (2010). *Nucleation in Condensed Matter: Applications in Materials and Biology*. Amsterdam: Elsevier.

19 Rodrigues, B.P. and Zanotto, E.D. (2012). Evaluation of the guided random parametrization method for critical cooling rate calculations. *J. Non-Cryst. Solids* 358: 2626–2634.

20 Zanotto, E.D., Tsuchida, J.E., Schneider, J.F., and Eckert, H. (2015). Thirty-year quest for structure-nucleation relationships in oxide glasses. *Int. Mater. Rev.* 60: 376–391.

21 Johari, G.P. and Schmelzer, J.W.P. (2014). Crystal nucleation and growth in glass-forming systems: some new results and open problems. In: *Glass: Selected Properties and Crystallization* (ed. J.W.P. Schmelzer), 531–590. Berlin: de Gruyter.

22 Kauzmann, W. (1948). The nature of the glassy state and the behavior of liquids at low temperatures. *Chem. Rev.* 43: 219–256.

23 Zanotto, E.D. and Cassar, D.R. (2018). The race within supercooled liquids – Relaxation versus crystallization. *J. Chem. Phys.* 149: 024503.

24 Schmelzer, J.W.P., Abyzov, A.S., Fokin, V.M. and Schick, C. (2018). Kauzmann paradox and the crystallization of glass-forming melts. *J. Non-Cryst. Solids* 501: 21–35.

25 Schmelzer, J.W.P. and Schick, C. (2012). Dependence of Crystallization Processes of Glass-forming Melts on Prehistory: A Theoretical Approach to a Quantitative Treatment. *Phys. Chem. Glasses B* 53: 99–106.

Note

Reviewers: E. Bellini Ferreira, University of São Paulo, São Carlos, SP, Brazil

F.C. Serbena, State University of Ponta Grossa, Paraná, Brazil